

# Mass/heat transfer coefficient in the radially rotating circular channels of the rotor of the high-speed heat regenerator

Joanna Wilk

*Thermodynamics Department, Rzeszów University of Technology, ul. W. Pola 2, 35-959 Rzeszów, Poland*

Received 20 June 2003

## Abstract

Laminar forced convection heat transfer in radially rotating circular channels of the rotor of the high-speed heat regenerator has been investigated. Mean values of the convective mass/heat transfer coefficient in these channels were measured electrolytically.

The measurements were made for  $Ro = 0.1$  and  $Ro = 0$ , in the range of Reynolds number from 250 to 1200. The value of Rossby number and the range of Reynolds number result from the hydraulic characteristics of the regenerator.

Finally, the correlations have been formulated for Chilton–Colburn coefficient vs. Reynolds number and for Nusselt number vs. Reynolds number.

In order to estimate the error of the heat transfer coefficient resulting from application of the mass/heat transfer analogy, a comparison of experimental thermal investigation, mass transfer experiments using electrolytic technique and theoretical analysis results has been performed in some defined cases.

© 2003 Elsevier Ltd. All rights reserved.

## 1. Introduction

Heat transfer in rotating ducts is an important subject in the study of technology for rotating machines e.g. cooling channels in gas turbines or heat transfer in rotors of modern high-speed heat exchangers.

In the radially rotating ducts, the rotationally induced Coriolis and centrifugal forces are generated and consequently affect the heat transfer and flow characteristic. The secondary flow formed this way is conducive to the heat transfer rate.

The problem of heat transfer coefficient in rotating channels, as an issue applicable in research and analysis of fluid-flow machines, has been undertaken by many authors.

The basic criteria by which papers concerning the  $\alpha$  coefficient can be classified, are the geometry of rotating channels and magnitude of Reynolds number characterising the flow in the channel.

There exists a number of papers dealing with heat transfer in rotating channels of square or rectangular cross-section for both turbulent and laminar flows occurring in the channel (cf. [1,2]). Examples of other papers dealing with the convection heat transfer coefficient in rotating circular tube for turbulent or laminar flows are, among others, [3–7].

The papers mentioned above concern research on convection heat transfer intensity in rotating channels. Based on those works, one may estimate parameters having fundamental effect on magnitude of heat transfer coefficient, which are: the above mentioned Reynolds number, the  $Ro$  number representing the ratio of Coriolis forces to inertial forces, the number  $Ra_{\omega}^* = Ra_{\omega}/Re^2$  representing the ratio of buoyancy forces related to density distribution patterns to inertial forces, and the geometry of the rotating channel, including the shape of transversal cross-section (geometrical shape coefficient, e.g. ratio of rectangle sides lengths), and ratio of the channel length to its hydraulic diameter.

In the present study, forced convection mass/heat transfer in radially rotating circular channels of porous

*E-mail address:* [joanwilk@prz.rzeszow.pl](mailto:joanwilk@prz.rzeszow.pl) (J. Wilk).

### Nomenclature

$A_k$	surface area of the cathode	$Ra_\omega$	rotational Rayleigh number
$C$	concentration of reacting ions	$Re$	Reynolds number, $wd/\nu$
$C_b$	bulk concentration of ferricyanide ions	$Ro$	Rossby number, $\omega d^2/w$
$C_w$	concentration of ions at the surface of electrode	$Sc$	Schmidt number, $\nu/D$
$D$	diffusivity of ferricyanide ions in the electrolyte	$Sh$	Sherwood number, $\beta d/D$
$D_1, D_2$	inner and outer diameter of the rotor	$St_H$	Stanton number for heat transfer, $\alpha/(c_{pg}\rho_g w_g)$
$d$	diameter, diameter of the rotating channel	$St_M$	Stanton number for mass transfer, $\beta/w$
$d_h$	hydraulic diameter	$U$	voltage
$F$	Faraday constant	$w, w_g$	mean velocity of electrolyte and gas, respectively
$I$	current in the circuit	$y$	normal coordinate
$i$	current density		
$i_p$	plateau current density		
$j_M, j_H$	Chilton–Colburn coefficient for heat and mass transfer, respectively	<i>Greek symbols</i>	
$n$	valence charge of reacting ions	$\alpha$	heat transfer coefficient
$N$	ions density flux	$\beta$	mass transfer coefficient
$l$	channel length	$\bar{\delta}$	mean thickness of Nernst diffusion layer
$L$	width of the rotor	$\nu$	kinematic viscosity of electrolyte
$Pr$	Prandtl number	$\rho, \rho_g$	density of electrolyte and gas, respectively
		$\omega$	angular velocity

rotor is investigated using electrolytic technique of heat/mass transfer analogy.

The paper describes experimental investigation with particular reference to its applications to the design of cooled or heated porous rotors of the high-speed heat regenerators.

A high-speed heat regenerator is a combination of two flow devices—a fan and a heat exchanger. Its fundamental part consist of a cylindrical porous rotor driven from the outside, inside which there is a fixed diaphragm separating a cold gas stream from a hot one. The rotor revolving with a high speed causes suction of the hot and cold gas from the opposite sides of the exchanger, then heating and cooling of the cold and hot gas, respectively, and at last it forces these gas streams through symmetrical outlet channels of the device housing.

A schematic diagram including basic construction details of such a device has been presented in [8]. As for the detailed description of a high-speed heat exchanger, it has been presented in papers [9,10], in which results of theoretical and experimental examinations of the device prototype are demonstrated.

A model rotor adopted for the electrolytic experimental research in this work had a porous structure formed by radially oriented ducts of a constant circular cross-section. Results of research concerning the  $\alpha$  coefficient carried out by means of the same method and for similar regenerator but of quite different rotor construction and rotor channels geometry, were presented in [11–13].

## 2. Experimental technique

The electrolytic technique consists in observation of the so-called controlled diffusion of ions, presumably at the cathode. Once the external voltage is applied to anode and cathode immersed in the electrolyte, the electric current arises in the external circuit, magnitude  $I$  of which, according to Faraday's law, shall be

$$I = nFA_k N \quad (1)$$

With the diffusion transport only taken into account, the ions density flux  $N$ , according to the Fick's law, equals

$$N = -\frac{DdC}{dy} \quad (2)$$

Then, making use of the Nernst's model well-known in electrochemistry (linear variation of concentration of ions vs. distance from the electrode surface in the diffusion layer) one may write

$$\frac{dC}{dy} = \frac{C_b - C_w}{\bar{\delta}} \quad (3)$$

and

$$\bar{\delta} = \frac{D}{\beta} \quad (4)$$

Based on Eqs. (1)–(4) one obtains

$$\frac{I}{A_k} = i = nF\beta(C_b - C_w) \quad (5)$$

Increase of the potential of the probe electrode results in increase of the transition reaction rate and in related decrease of concentration of ions at the surface of the electrode and, as a consequence, in increase of the electric current in the external circuit. If the surface of the anode is much greater than this of the cathode, then, with successive increase of the external voltage, one arrives at conditions at which  $C_w = 0$  at the cathode (controlled diffusion). Further increase of the electrode potential does not result in increase of the current, which reaches the value of the so-called plateau current  $I_p$ . The current density  $i_p$  is then used for calculations of the mass exchange coefficient  $\beta$  according to the relation

$$\beta = \frac{i_p}{nFC_b}. \quad (6)$$

### 3. Apparatus

The measurements have been performed at the universal rig, described in details in [11,12]. The scheme of the rig is presented in Fig. 1.

Nickel electrodes in aqueous solution of equimolar quantities of  $K_3Fe(CN)_6$  and  $K_4Fe(CN)_6$  in the presence of 1 M NaOH basic solution have been applied.

Presence of the NaOH-based electrolyte in the hydraulic system required application of special materials

like PVC, acid resistant steel and electrolyte resistant rubber.

The exchangeable element of the set-up was the measurement section representing the model of the regenerator, including the model of the rotor with nickel surfaces of several channels (cathodes) at which measurements of mass/heat transfer coefficients were taken. The anode consisted in two nickel plates connected in parallel and glued to external surfaces of exhaust collectors of the measurement section.

In the course of measurements with the rotating rotor model, an additional specially designed system was applied consisting of three-phase electric motor of SG-122M-8 type driving the rotor, and frequency converter (inverter) of AMT 0004/RN 513 type. The rotational speed was controlled by means of the NT-1-AR SM speed indicator.

The measurement stand enabled for: stabilisation and measurement of the temperature, release of oxygen from the electrolyte by means of washing with nitrogen, step alteration and measurement of the external voltage applied to the electrodes, and measurement of electric current in external circuit.

The contact with the cathodes was provided by means of electrical collector rings.

In Fig. 2, a scheme of the cylindrical rotor model is presented with radially drilled capillary channels of diameters  $d = 1.5$  mm. The rotor has been made of PVC. Four channels have been reamed and nickel tubes of internal diameter 1.5 mm placed inside, internal surface of which serving as the cathode. Parameters of the

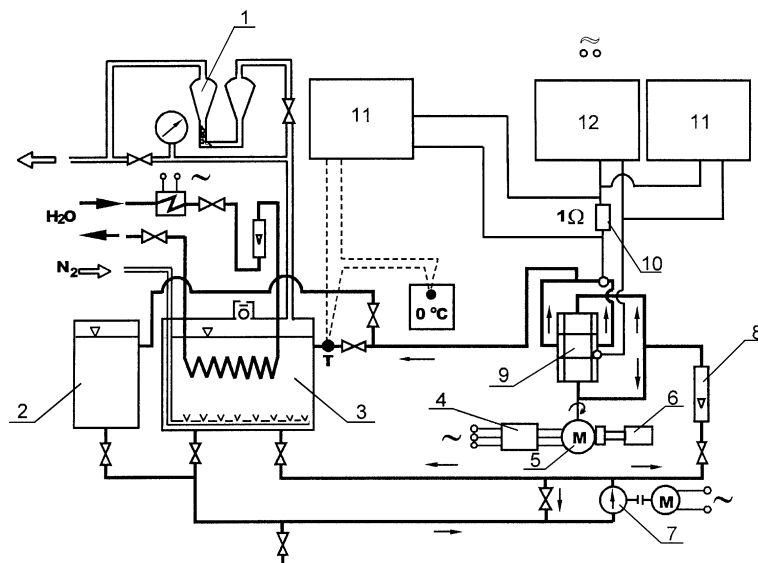


Fig. 1. Scheme of the rig: 1—visual control of  $N_2$  flux, 2—tank with electrolyte for activation, 3—main tank with cooling coil, 4—inverter, 5—driving motor, 6—angular rate sensor, 7—pump, 8—rotameter, 9—test section, 10—standard resistor, 11—digital millivoltmeter.

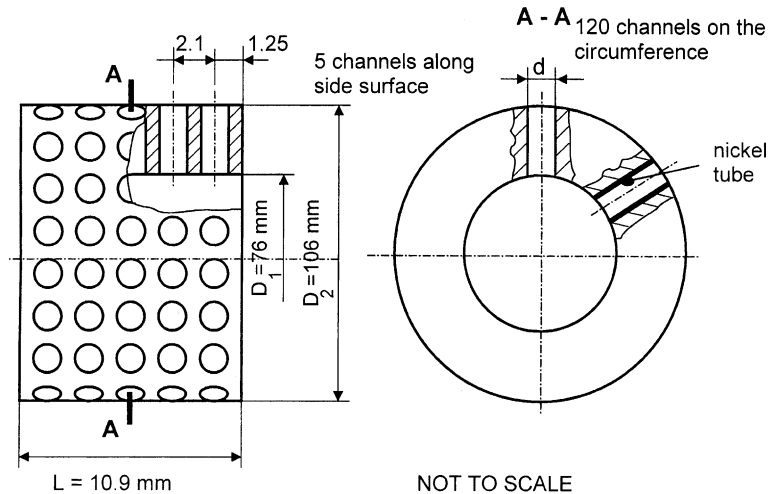


Fig. 2. Scheme of the porous rotor.

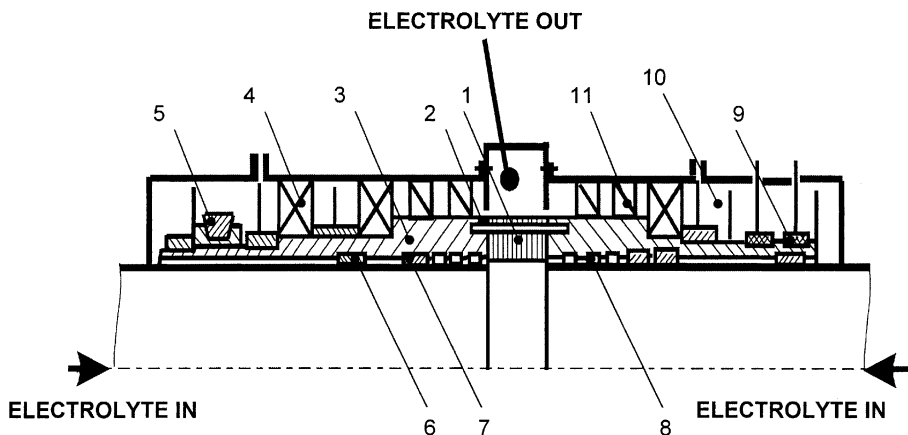


Fig. 3. Scheme of the test section: 1—porous rotor with radial circular channels, 2—driving pin, 3—hub, 4—ball bearing, 5—V-belt, 6—spacer ring, 7—O-ring seal, 8—labyrinth seal, 9—collector ring, 10—thrower, 11—sink.

rotor model, such as external and internal diameters, as well as the porosity equal to 0.345, were the same as those of the actual rotor tested in [10]. The model of the rotor have been installed in specially designed section [12], schematic diagram of which is presented in Fig. 3.

## 4. Results and discussion

### 4.1. Results of measurements

In order to maintain the similarity between phenomena of the gas flow in channel of the actual rotor and of the electrolyte flow in channels of the rotor model, equality of Reynolds numbers has been assured.

Analogy between mass forces was kept by means of equality of Rossby numbers.

The range of Reynolds numbers (250–1200) and the value of  $Ro = 0.1$  result from the hydraulic characteristics of the actual heat exchanger of the same external dimensions, rotor structure, and porosity as in the model under examination, which has been described in [10].

As the result of the performed measurements, polarisation curves have been obtained with apparently flat sections, examples of which are presented in Fig. 4. Based on these graphs, values of controlled diffusion current  $I_p$  have been determined, which in turn allowed for calculation of values of the mass transfer coefficient  $\beta$

$$\beta = \frac{I_p}{A_k F C_b} \quad (7)$$

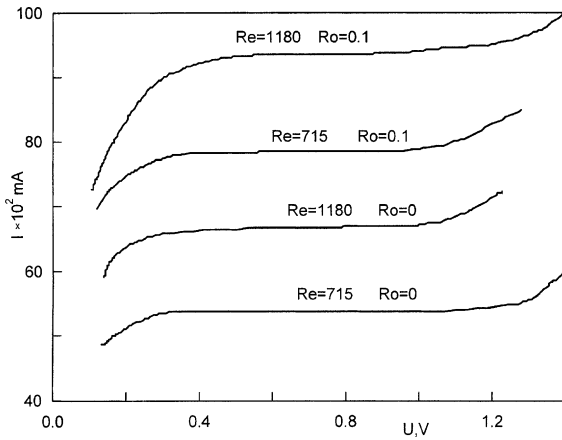


Fig. 4. Examples of the polarization curves.

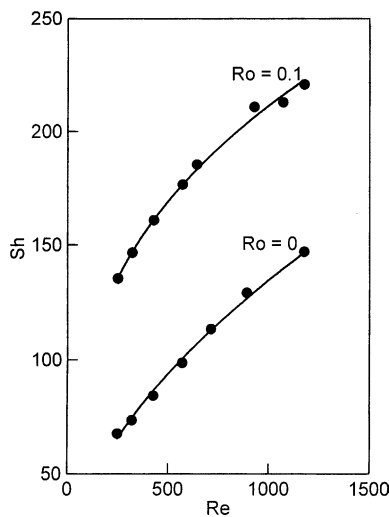


Fig. 5. Final results on  $Sh$  vs.  $Re$  at parameter  $Ro$ .

and of the Sherwood number

$$Sh = \beta d / D \tag{8}$$

(taking into account that  $n = 1$ ).

In Fig. 5, the dependence of  $Sh$  number on  $Re$  is presented for  $Ro = 0$  (without rotation) and for  $Ro = 0.1$ .

#### 4.2. Mass and heat transfer analogy

There exists the exact analogy between mass and heat transfer in case of movable and immovable fluids. In mass transfer by means of diffusion, fundamental role is played by concentration gradient of the exchanged molecules or ions, while in exchange of heat—by the gradient of temperature of the fluid. Similar terminology and mathematical models are being used for description of both exchange processes. And thus, for mass transfer

related to forced convection, the solution of the problem is presented in the general form

$$Sh = Sh(Re, Sc) \tag{9}$$

analogously, for heat transfer,

$$Nu = Nu(Re, Pr) \tag{10}$$

In case of occurrence of rotation, one has to introduce additionally the  $Ro$  number into Eqs. (9) and (10), which gives

$$Sh = Sh(Re, Ro, Sc) \tag{11}$$

and

$$Nu = Nu(Re, Ro, Pr) \tag{12}$$

In the present paper, the Chilton–Colburn correlation has been applied in the form

$$j_M = St_M Sc^{2/3} \tag{13}$$

$$j_H = St_H Pr^{2/3} \tag{14}$$

$$j_M = j_H \tag{15}$$

where:  $j_M$ ,  $j_H$ —Chilton–Colburn coefficients for mass and heat transfer adequately.

Results of experiments are presented in the form of the correlation  $j_M = f(Re)$  with  $Ro$  being a parameter, where  $j_M$  is the value of the coefficient averaged along length and perimeter of the channel. Material data for the electrolyte at temperature 25 °C, necessary for determination of the  $j_M$  coefficient, were as follows:  $D = 6.71 \times 10^{-10} \text{ m}^2/\text{s}$ ,  $\nu = 1.145 \times 10^{-6} \text{ m}^2/\text{s}$ .

Velocity of the electrolyte resulted from the assumed electrolyte flux.

Mean values of  $j_M$  for rotating channel, obtained by means of electrolytic measurements, are presented in Fig. 6. In order to estimate the effect of rotation on

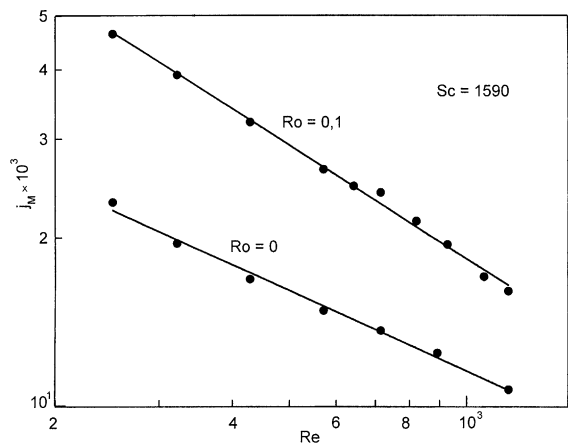


Fig. 6. Graphical presentation of correlations on  $j_M$  vs.  $Re$  at  $Ro = 0$  and  $Ro = 0.1$ .

intensification of exchange processes, values of  $j_M$  without rotation have been also presented in Fig. 6.

Dependence of  $j_M$  vs.  $Re$  can be described by means of correlations

$$j_M = 0.31Re^{-0.48} \quad (16)$$

for  $Ro = 0$ , and

$$j_M = 1.93Re^{0.67} \quad (17)$$

for  $Ro = 0.1$ .

Eqs. (13)–(15) and 16,17 served as a basis for determination of correlations describing dependence of average Nusselt number  $Nu$  vs.  $Re$ :

$$Nu = 0.275Re^{0.52} \quad (18)$$

for  $Ro = 0$ , and

$$Nu = 1.714Re^{0.33} \quad (19)$$

for  $Ro = 0.1$ .

#### 4.3. Comparison of experimental results with other authors' data

Investigations concerning heat transfer in rotating circular capillary channel of high-speed rotating heat exchanger are, in principle, unprecedented in the literature. Therefore, results of our own research have been compared to existing data concerning heat transfer for other types of channels in rotors of similar types and for single circular channel of similar  $l/d$  ratio and  $Re$  and  $Ro$  numbers. Results of the comparison are summarised in Fig. 7.

Fig. 8, in turn, represents comparison of research results concerning heat transfer intensification rate by means of introduction of the  $Nu_r/Nu_s$  ratio, where:  $Nu$ —mean Nusselt number in rotation conditions and  $Nu_s$ —in static conditions respectively.

For our own research results represented in Fig. 8 by curve no. 1, the  $Nu_r/Nu_s$  ratio decreases together with increase of  $Re$  number, which is the evidence of reduction of the effect of Coriolis force on mass/heat transfer intensity with increasing Reynolds number. Similar decreasing trend towards increasing  $Re$  number is observed in curve no. 2 representing experimental results for single circular channel [4]. Magnitude of the  $Nu_r/Nu_s$  ratio in this case is, however, much less than in the case of circular channel of regenerator's rotor. Rate of mass/heat transfer intensification for rotors of other types (curves nos. 3 and 4) is also less than this for the rotor with radial circular channels.

One has to admit that in case of analogy experiments described in this paper, intensification of mass/heat transfer was caused only by action of Coriolis forces. Because of isothermality of the measurement, buoyancy forces have not occurred.

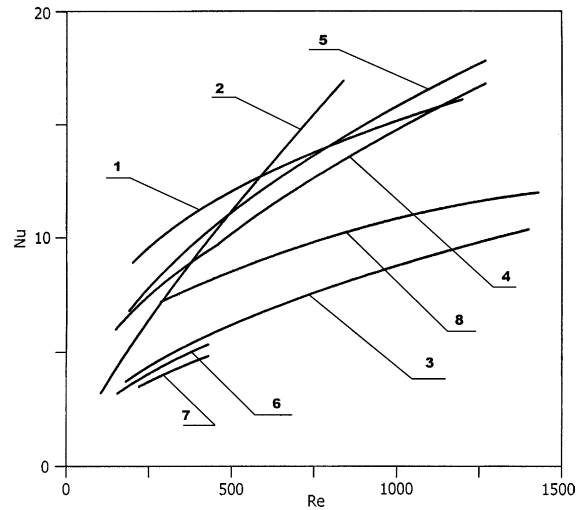


Fig. 7. Comparison of present mass/heat transfer data in rotating channel with previous research: 1—present electrolytical research for circular channel of the rotor;  $l/d = 10$ ,  $d_h = d = 1.5$  mm,  $Ro = 1$ ; 2—results of thermal balance method for curved and diffusor-like channel of the rotor,  $d_h = 2.6$  mm,  $Ro = 0.12$  [10]; 3—as above,  $d_h = 1.5$  mm,  $Ro = 0.2$ ; 4—electrolytical research of curved and diffusor-like channel of the rotor,  $d_h = 2.26$  mm,  $Ro = 0.15$  [13]; 5—as above at  $Ro = 0.2$ ; 6—electrolytical research of curved and diffusor-like channel of the rotor,  $d_h = 1.17$  mm,  $Ro = 0.12$  [12]; 7—as above at  $Ro = 0.08$ ; 8—thermal research of single circular channel,  $l/d = 6$ ; 12; 24 (one curve),  $Ro = 0.1$  [4].

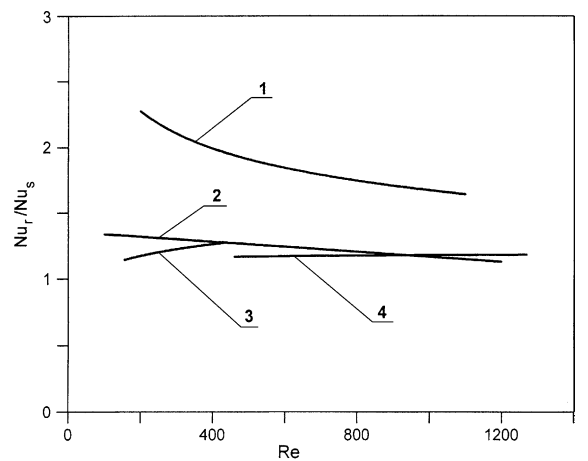


Fig. 8. Rate of increase of  $Nu$  in comparison with the stationary case (at  $Ro$  near-0.1): 1—present electrolytical research for circular channel of the rotor;  $l/d = 10$ ,  $d_h = d = 1.5$  mm; 2—thermal research of single circular channel,  $l/d = 6$ , 12 and 24 (one curve) [4]; 3—electrolytical research of curved and diffusor-like channel of the rotor,  $d_h = 2.26$  mm [13]; 4—electrolytical research of curved and diffusor-like channel of the rotor,  $d_h = 1.17$  mm [12].

**5. Analysis of experimental method accuracy**

*5.1. Measurement error of the mass transfer coefficient*

Average relative errors of composite quantities  $y = y(x_1, x_2, \dots, x_i)$  were calculated according to the general relation

$$\left| \frac{\Delta y}{y} \right| = \sqrt{\sum_{i=1}^n \left( \frac{\partial y}{\partial x_i} \Delta x_i \right)^2} \quad (20)$$

The mass transfer coefficient  $\beta$  has been derived from Eq. (6).

The relative error of measurement of  $\beta$  equals

$$\left| \frac{\Delta \beta}{\beta} \right| = \sqrt{\left( \frac{\Delta I_p}{I_p} \right)^2 + \left( \frac{\Delta A_k}{A_k} \right)^2 + \left( \frac{\Delta C_b}{C_b} \right)^2} \quad (21)$$

The measurement of the following quantities account for the above errors: concentration  $C_b$ , plateau current  $I_p$ , and cathode surface area  $A_k$ .

Concentration of ferricyanide ions in the electrolyte has been determined by means of the titration method hence  $|\Delta C_b/C_b| = 1.4\%$ .

The plateau current measurement has been done by means of digital millivoltmeter, therefore  $|\Delta I_p/I_p| = 0.1\%$  is the error resulting from the instrument's class of accuracy (measurement of the voltage drop at the standard resistance).

The average error of determination of the cathode surface area was estimated as  $|\Delta A_k/A_k|$  and resulted from adopted relative error of measurement of the nickel tube internal diameter equal to 0.07%.

After substitution of respective data to the formula given by Eq. (21), the relative error of the mass transfer coefficient  $|\Delta \beta/\beta|$  has been estimated as 1.6%.

*5.2. Error of determination of Chilton–Colburn coefficient*

Error of determination of the  $j_M$  coefficient has been derived from the relation (based on Eqs. (20) and (13))

$$\left| \frac{\Delta j_M}{j_M} \right| = \sqrt{\left( \frac{2\Delta Sc}{3Sc} \right)^2 + \left( \frac{\Delta St_M}{St_M} \right)^2}, \quad (22)$$

where:  $|\frac{\Delta Sc}{Sc}| = 7\%$  [3] and  $|\frac{\Delta St_M}{St_M}| = \sqrt{\left( \frac{\Delta \beta}{\beta} \right)^2 + \left( \frac{\Delta w}{w} \right)^2}$ .

Because of large difference between maximum and minimum error of determination of the electrolyte flow velocity through the capillary channel  $|\Delta w/w|$ , other specific errors have been determined for both cases.

After substitution of respective data one obtains:

$$\left| \frac{\Delta j_M}{j_M} \right|_{\max} = 8.6\% \quad \text{and} \quad \left| \frac{\Delta j_M}{j_M} \right|_{\min} = 5.2\%.$$

*5.3. Error of the correlations*

Correlations described with formulae of Eqs. (16) and (17) have been determined by means of the least squares method. The error of the correlation given by Eq. (17) describing the case with rotation, has been calculated by means of statistical method assuming normal distribution of deviations between measurement results and correlation curve. The error equals 0.17%. Because of its small value in comparison with the error of determination of the Chilton–Colburn coefficient, it is practically meaningless.

*5.4. Error of the analogy*

In order to estimate the error of the heat transfer coefficient resulting from application of the mass/heat transfer analogy, a comparison of experimental heat tests, mass transfer experiments using electrolytic technique and theoretical analysis results has been performed in some defined cases.

As a base for these comparisons, we used electrolytic mass transfer test in circular pipe presented in [14] and our own results of electrolytic test for immovable circular capillary channel of regenerator's rotor.

On the grounds of correlations describing functions  $j_M(Re)$  given in [14] for two ranges of  $Re$  number, we have defined relations  $Nu(Re)$  using the Chilton–Colburn analogy. In the calculations, the value of  $Pr = 0.7$  has been adopted. Obtained curves are presented in Figs. 9 and 10 for selected values of the  $l/d$  ratio.

Within the range of values of  $Re \in (6000, 12,600)$ , the results are compared to those obtained according to theoretical analysis of turbulent developing heat transfer [15] and to the relation given by Michiejew [16] for similar  $l/d$  ratio with the effect of pipe length taken into account.

It can be seen that there exist a good consistence between compared results within the considered range of  $Re$  numbers, and maximum difference between them calculated by means of the general relation is

$$\Delta Nu = \frac{Nu^* - Nu_{an}}{Nu_{an}} \times 100\% \quad (23)$$

where,  $Nu_{an}$ —mean Nusselt number obtained by means of Chilton–Colburn analogy with use of electrolytic method,  $Nu^*$ —mean Nusselt number obtained otherwise than  $Nu_{an}$  for similar case.

In Fig. 10, relation  $Nu(Re)$  obtained based on mass/heat transfer analogy (for  $l/d = 1.56$ ) [14] is compared to relations given by Deissler [17] and Michiejew [16] (for  $l/d = 2$ ), as well as to results of the theoretical analysis according to [15]. Some other results of thermal investigation [7], which significantly differ from the others, are also presented.

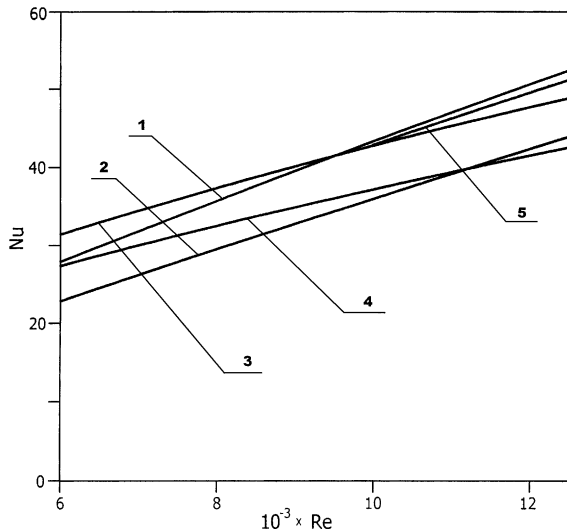


Fig. 9. Heat transfer in entrance region of the circular pipe,  $Re \in (6000, 12,700)$  (the range of  $Re$  conditioned by electrolytical research): 1—electrolytical research,  $l/d = 1.56$  [14]; 2—electrolytical research,  $l/d = 2.61$  [14]; 3—theoretical prediction for heat transfer in entrance region,  $l/d = 1.56$  [15]; 4—as above,  $l/d = 2.61$ ; 5—relation given by Michiejew,  $l/d = 2$ ,  $10,000 < Re < 20,000$  [16].

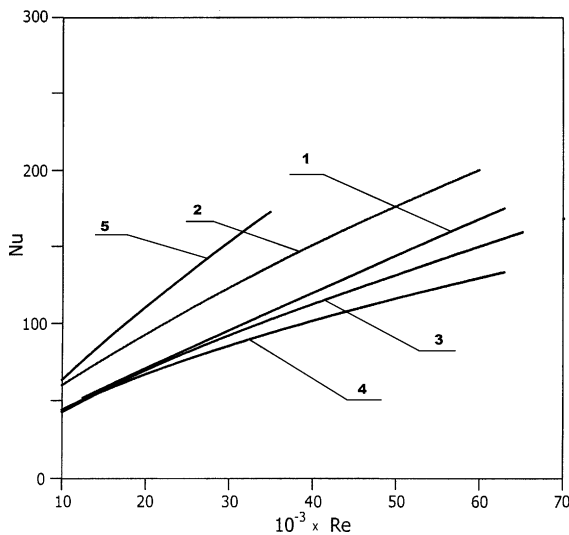


Fig. 10. Heat transfer in entrance region of the circular pipe in the case of turbulent flow: 1—electrolytical research,  $l/d = 1.56$  [14]; 2—according to Deissler,  $l/d = 2$  [14]; 3—according to Michiejew,  $l/d = 2$  [16]; 4—theoretical prediction for heat transfer in entrance region,  $l/d = 1.56$  [15]; 5—thermal research,  $l/d = 1.56$  [7].

Curves nos. 1, 3, and 4 representing respectively: results of the electrolytical tests, and relations given by Michiejew and by Madejski, are, in principle, confor-

mant within the range of  $Re \in (10,000, 20,000)$ . With increasing  $Re$  number, the difference between them becomes greater. Maximum deviation between results of electrolytical tests and results given by Michiejew is of order of 11%. Similar comparison with results obtained based on theoretical solution given by Madejski leads to the maximum deviation of 25%. The curve no. 2 (according to Deissler) in the whole range of Reynolds numbers is deviated from curve no. 1 by some  $-20\%$ .

At Fig. 11, the dependence of  $Nu$  number on  $Re$  for convection heat transfer at laminar gas flow through a circular pipe is presented. The curve no. 1 represents results of our own electrolytical tests adopting the Chilton–Colburn analogy. The results were obtained for rotor’s single channel ( $l/d = 10$ ) in stationary conditions (without rotation). The curve no. 3 represents dependence given by Kays, valid for gas flow at  $Pr = 0.7$ , within the interval of hydraulic stabilisation, with constant temperature of the wall being assumed [18]. Next, curve no. 4 represents an expression for the heat exchange according to empirical formula of Sider Tate [19], and curve no. 5—theoretical equation given by L ev eque [20] for the developing heat transfer. The curve no. 2 represents results of heat tests based on [4], performed for values of  $l/d = 6, 12$ , and  $24$ . The presented result is an average. It can be seen that, in case of laminar flow, results of electrolytical test are in excellent consistence with results of heat tests according to [4].

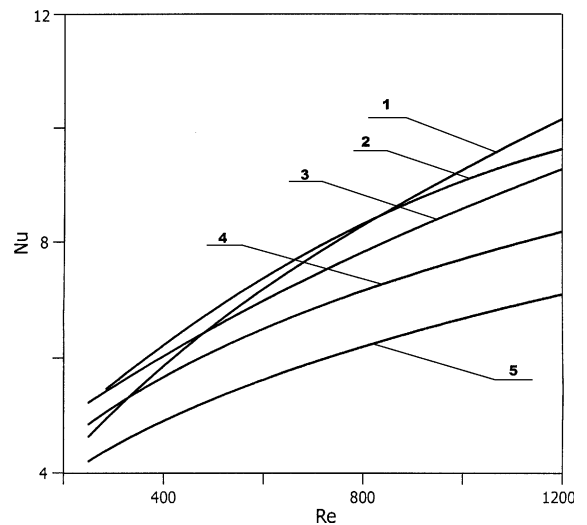


Fig. 11. Heat transfer in entrance region of the circular pipe in the case of laminar flow: 1—present electrolytical research for circular channel of the rotor in the stationary conditions,  $l/d = 10$ ; 2—thermal research, values of  $Nu$  averaging for  $l/d = 6, 12$  and  $24$  [4]; 3—according to Kays,  $l/d = 10$ , constant wall temperature [18]; 4—according to Sider-Tate,  $l/d = 10$  [19]; 5—according to L ev eque [20].



Deviations  $\Delta Nu$ , calculated according to Eq. (23), are as follows in this case: +7% for  $Re = 400$ , 0% for  $Re = 850$ , and -6% for  $Re = 1200$ . There is also a good consistency with the solution given by Kays [18].

The other curves in Fig. 11 (nos. 4 and 5) differ significantly from the curve no. 1. This can follow from the fact that electrolytic tests have been performed for the channel of very small length and diameter (a capillary channel). One should hardly expect, in this case, the consistency of experimental results with theoretical analysis concerning gas flow through straight-line axial channel of typical dimensions.

Concluding, one can assume that, based on examples given above, there exist rather good consistency of calculations results obtained for the heat interception coefficient related to flow through a circular channel by means of electrolytic technique, with the results obtained on the grounds of theoretical analysis or thermal tests. Results of the comparison are good especially for small values of Reynolds number.

Another problem, examination of which served in the present paper as an attempt to estimate the error of the mass/heat transfer analogy, was the industrial process of heating of the batch in metallurgical furnace. The problem has been considered in [21], where the comparison of results obtained by means of heat, electrolytic, and naphthalene test, has been carried out. The authors have approximated results of tests obtained by means of all three methods and obtained a single curve of the form  $j = 0.206Re^{-0.38}$ , where  $j$  is the Chilton–Colburn coefficient. In their summary, the authors noted that results of measurements obtained by means of all three methods, for various dimensions of the batch, within the 57% of the  $Re$  range go into the band of  $\pm 10\%$ , and within 98% of the  $Re$  range—to the band of  $\pm 25\%$ . Taking into account measurement errors related to the specific technique one may note a very good consistency of mass/heat transfer test results obtained with all three methods.

Determination of the actual value of the error of the applied analogy method on the grounds of comparisons carried out in the present section, is a very difficult issue. Taking into account all facts discussed herein, one may attempt to conclude that the mass/heat transfer analogy error is of the same order of magnitude as the error of determination of the  $\alpha$  coefficient by means of a specific measuring technique.

## 6. Conclusions

As a result of the experimental investigation of mass/heat transfer coefficients in rotating circular channels of the high-speed regenerative heat exchanger rotor the following conclusions can be formulated:

- a substantial effect of body forces on the mass/heat transfer coefficient in rotating channels is observed;
- as the electrolytic measurements are isothermal, the convective mass transfer has been affected by secondary flows only from Coriolis force;
- correlations describing laminar forced convective mass/heat transfer in thin circular channels with and without rotation are different than those for normally sized channels;
- error of mass/heat transfer analogy obtained on the basis of comparison of heat and mass transfer research results and theoretical predictions in same cases is of the same order of magnitude as the error of determination of the  $\alpha$  coefficient by means of a specific measuring technique.

## Acknowledgements

The author would like to express the gratitude to Prof. Bogumił Bieniasz for his help and great interest in the experiment.

## References

- [1] T.C. Jen, A.S. Lavine, Laminar heat transfer and fluid flow in the entrance region of a rotating duct with rectangular cross section: The effect of aspect ratio, Transactions of ASME, Journal of Heat Transfer 114 (1992) 574–581.
- [2] C.Y. Soong, S.T. Lin, G.J. Hwang, An experimental study of convective heat transfer in radially rotating rectangular ducts, Transactions of ASME, Journal of Heat Transfer (1991) 604–611.
- [3] G.J. Hwang, T.C. Jen, Convective heat transfer in rotating isothermal ducts, International Journal of Heat and Mass Transfer 33 (9) (1990) 1817–1828.
- [4] D.E. Metzger, R.L. Stan, Entry region heat transfer in rotating radial tubes, AIAA Paper (1977) 1–6.
- [5] Y. Mori, W. Nakayama, Convective heat transfer in rotating radial circular pipes (1st report, laminar region), International Journal of Heat and Mass Transfer 11 (1968) 1027–1040.
- [6] Y. Mori, T. Fukada, W. Nakayama, Convective heat transfer in a rotating radial circular pipe (2nd report), International Journal of Heat and Mass Transfer 14 (1971) 1807–1824.
- [7] W.D. Morris, S.W. Chang, Heat transfer in a radially rotating smooth-walled tube, The Aeronautical Journal (1998) 277–285.
- [8] J.R. De Fries, Heat exchanger, Patent USA No. 3456718, 1969.
- [9] W. Wawszczak, Experimental investigation of a modern high rotating heat exchanger, Proceedings of the ASME Conference on Engineering Systems Design and Analysis, vol. 8, part C, London, 1994, pp. 679–686.
- [10] W. Wawszczak, High rotating heat exchanger, Scientific Bulletin of Łódź Technical University 705, Łódź, 1994.

- [11] B. Bieniasz, J. Wilk, Forced convection mass/heat transfer coefficient at the surface of the rotor of the sucking and forcing regenerative exchanger, *International Journal of Heat and Mass Transfer* 38 (10) (1995) 1823–1830.
- [12] B. Bieniasz, Heat transfer coefficient for porous regenerator rotor at gas flow modified by body forces due rotation, *Archives of Thermodynamics* 20 (3–4) (1999) 89–103.
- [13] B. Bieniasz, Influence of rotation of the regenerator rotor, made of corrugated sheets, on convective mass/heat transfer coefficient, in: *Proceedings of the 8th International Symposium: Heat Transfer and Renewable Energy Sources, Szczecin-Łeba 2000*, pp. 39–46.
- [14] B. Bieniasz, Mass transfer in the entrance region of a pipe, *Archives of Thermodynamics* 12 (1–4) (1991) 117–129.
- [15] J. Madejski, *Heat Transfer Theory*, Publishing House of Technical University of Szczecin, Szczecin, 1998.
- [16] M.A. Michiejew, *Osnowy Tęplotyprędaczi*, third ed., GEI, Moscow, 1956.
- [17] R.G. Deissler, Analysis of turbulent heat transfer and flow in the entrance regions of smooth passages, NACA Technical Note 3016, 1953.
- [18] W.M. Kays, Numerical solutions for laminar flow heat transfer in circular tubes, *Transactions of the ASME Journal of Heat Transfer* 77 (1955) 1265–1272.
- [19] E.N. Sider, G.E. Tate, Heat transfer and pressure drop of liquids in tubes, *Industrial and Engineering Chemistry* 28 (1936) 1429–1436.
- [20] M.A. Lévêque, Les lois de la transmission de la chaleur par convection, *Annales des Mines* 13 (1928) 201–299, 305–362, 381–415.
- [21] D.M. Lucas, R.M. Davies, Mass transfer modelling techniques in the prediction of convective heat transfer coefficients in industrial heating processes, in: *Proceedings of Fourth International Heat Transfer Conference, Paris, Versailles, vol. VII, Paper MT 1.2.*, Elsevier, Amsterdam, 1970.